

Next-to-leading-order QCD corrections to the decay of Z boson into $\chi_c(\chi_b)$

Zhan Sun^{1*} and Hong-Fei Zhang^{2†}

¹ *Department of Physics, Guizhou Minzu University, Guiyang 550025, P. R. China.*

² *School of Science, Chongqing University of Posts and Telecommunications, Chongqing, China.*

(Dated: September 10, 2018)

Abstract

Based on the framework of nonrelativistic Quantum Chromodynamics (NRQCD), we carry out next-to-leading order (NLO) QCD corrections to the decay of Z boson into χ_c and χ_b , respectively. The branching ratio of $Z \rightarrow \chi_c(\chi_b) + X$ is about $10^{-5}(10^{-6})$. It is found that, for $Z \rightarrow \chi_c(\chi_b) + X$, the single gluon fragmentation diagrams of $^3S_1^{[8]}$, which first appear at the NLO level, can provide significant contributions, leading to a great enhancement on the leading-order results. Consequently the contributions from the color octet (CO) channels will account for a large proportion of the total decay widths. Moreover, the introduction of the CO processes will thoroughly change the color singlet (CS) predictions on the ratios of $\Gamma_{\chi_{c1}}/\Gamma_{\chi_{c0}}$, $\Gamma_{\chi_{c2}}/\Gamma_{\chi_{c0}}$, $\Gamma_{\chi_{b1}}/\Gamma_{\chi_{b0}}$ and $\Gamma_{\chi_{b2}}/\Gamma_{\chi_{b0}}$, which can be regarded as an outstanding probe to distinguish the CO and CS mechanism. With regard to the CS ($^3P_J^{[1]}$) channels, the heavy quark pair associated processes serve as the leading role, however, in the case of χ_b , $Z \rightarrow b\bar{b}[^3P_J^{[1]}] + g + g$ can also contribute significantly. Summing over all the feeddown contributions from χ_{cJ} and χ_{bJ} , respectively, we find $\Gamma(Z \rightarrow J/\psi + X)|_{\chi_c\text{-feeddown}} = (0.28 - 2.4) \times 10^{-5}$ and $\Gamma(Z \rightarrow \Upsilon(1S) + X)|_{\chi_b\text{-feeddown}} = (0.15 - 0.49) \times 10^{-6}$.

PACS numbers: 12.38.Bx, 12.39.Jh, 13.38.Dg, 14.40.Pq

*Electronic address: zhansun@cqu.edu.cn

†Electronic address: hfzhang@ihep.ac.cn

I. INTRODUCTION

As one of the most successful theories describing the production of heavy quarkonium, nonrelativistic Quantum Chromodynamics (NRQCD) [1] has proved its validity in many processes [2–13], including the hadroproductions of J/ψ , η_c and Υ , and the photo-/electro-productions of J/ψ etc. Despite these successes, NRQCD still faces many challenges, for example the NRQCD predictions significantly overshoot the measured total cross section of $e^+e^- \rightarrow J/\psi + X_{\text{non-}c\bar{c}}$ released from *BABAR* and Belle collaborations [14]; the J/ψ polarization puzzle is still under debate [15–17]. One key factor responsible for these problems is that there are three LDMEs to be determined, bringing about difficulties in fitting the LDMEs and drawing a definite conclusion.

In comparison with J/ψ , χ_c is more “clean”, namely at leading-order (LO) accuracy in v , $^3S_1^{[8]}$ is the unique color octet (CO) state involved, which is beneficial to carry out further study. In addition, considering the branching ratios of $\chi_c \rightarrow J/\psi + \gamma$ are sizeable, the χ_c feeddown may have a significant effect on the yield and/or polarization of J/ψ , for example the inclusion of the χ_c feeddown will evidently make the polarization trend of the hadroproduced J/ψ more transverse. On the experiment side, χ_c can be easily detected by hunting the ideal decay processes, $\chi_c \rightarrow J/\psi \rightarrow \mu^+\mu^-$. In conclusion, comparing to J/ψ , χ_c has its own advantages on further studying heavy quarkonium, deserving a separate investigation.

In the past few years, there have been a number of literatures concerning the studies of the χ_c and χ_b productions, mainly focusing on the hadroproduction processes [3–5, 8, 18–21]. Ma et al. [22] for the first time accomplished the next-to-leading order (NLO) QCD corrections to the χ_c hadroproductions. Later on Zhang et al. [23] carried out a global analysis of the copious experimental data on the χ_c hadroproduction, indicating that almost all the existing measurements can be reproduced by the NLO predictions based on NRQCD. To further check the validity and universality of the χ_c related LDMEs, it is indispensable to utilize them in other processes.

For this purpose, considering that copious Z boson events can be produced at LHC, the axial vector part of the Z -vertex allows for a wider variety of processes and the relative large mass of Z boson can make the perturbative calculations more reliable, we will, for the first time, perform a systematic study on the decay of the Z boson into χ_c within the framework

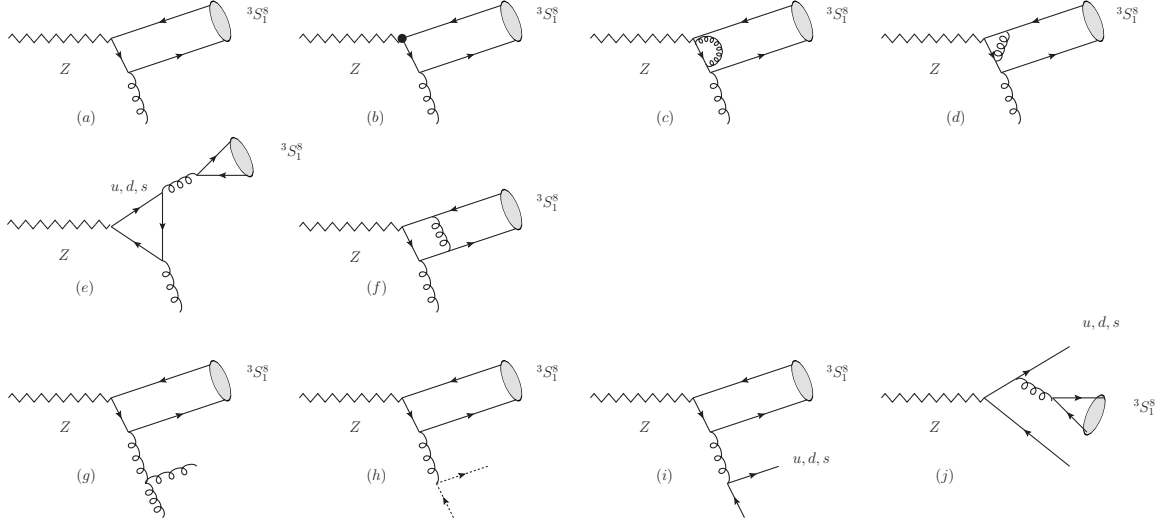


FIG. 1: Typical Feynman diagrams for the NLO processes of $^3S_1^{[8]}$.

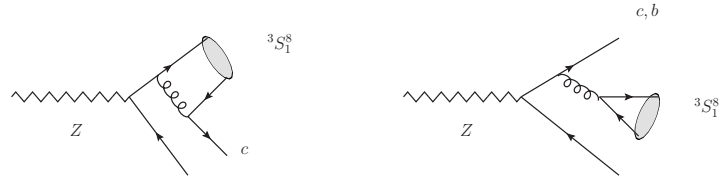


FIG. 2: Typical Feynman diagrams for the NLO* processes of $^3S_1^{[8]}$.

of NRQCD. Note that, due to the larger mass of the $b\bar{b}$ mesons, the typical coupling constant and relative velocity of bottomonium are smaller than those of charmonium, subsequently leading to better convergent results over the expansion in α_s and v^2 than the charmonium cases. Thus, in this article, the χ_b productions via Z boson decay will also be systematically investigated.

The rest paragraphs are organized as follows: In Sec. II we give a description on the calculation formalism. In Sec. III, the phenomenological results and discussions are presented. Sec. IV is reserved as a summary.

II. CALCULATION FORMALISM

Within the NRQCD framework, the decay width of $Z \rightarrow \chi_c(\chi_b) + X$ can be written as:

$$d\Gamma = \sum_n d\hat{\Gamma}_n \langle \mathcal{O}^H(n) \rangle \quad (1)$$

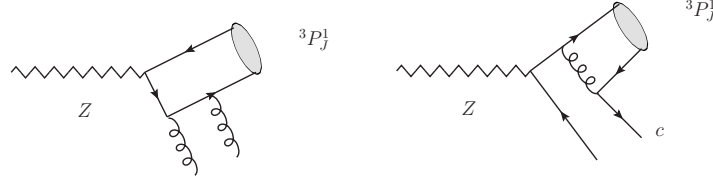


FIG. 3: Typical Feynman diagrams for the processes of ${}^3P_J^{[1]}$, namely $Z \rightarrow c\bar{c}[{}^3P_J^{[1]}] + g + g$ and $Z \rightarrow c\bar{c}[{}^3P_J^{[1]}] + c + \bar{c}$.

where $d\hat{\Gamma}_n$ refers to the perturbative calculable short distance coefficients, representing the production of a configuration of the $Q\bar{Q}$ intermediate state with a quantum number n , and $\langle\mathcal{O}^H(n)\rangle$ is the universal non-perturbative LDME. According to NRQCD, for χ_c and χ_b related processes, only two states should be taken into considerations at LO accuracy in v , namely ${}^3S_1^{[8]}$ and ${}^3P_J^{[1]}$. Taking χ_c as an example, up to $\mathcal{O}(\alpha\alpha_s^2)$, for $n = {}^3S_1^{[8]}$ we have

$$\begin{aligned}
\text{LO : } Z &\rightarrow c\bar{c}[{}^3S_1^{[8]}] + g, \\
\text{NLO : } Z &\rightarrow c\bar{c}[{}^3S_1^{[8]}] + g \text{ (virtual),} \\
&Z \rightarrow c\bar{c}[{}^3S_1^{[8]}] + g + g, \\
&Z \rightarrow c\bar{c}[{}^3S_1^{[8]}] + u_g + \bar{u}_g \text{ (ghost),} \\
&Z \rightarrow c\bar{c}[{}^3S_1^{[8]}] + u + \bar{u}, \\
&Z \rightarrow c\bar{c}[{}^3S_1^{[8]}] + d(s) + \bar{d}(\bar{s}), \\
\text{NLO* : } Z &\rightarrow c\bar{c}[{}^3S_1^{[8]}] + c + \bar{c}, \\
&Z \rightarrow c\bar{c}[{}^3S_1^{[8]}] + b + \bar{b},
\end{aligned} \tag{2}$$

and in the case of $n = {}^3P_J^{[1]}$, there are two involved channels as listed below:

$$\begin{aligned}
Z &\rightarrow c\bar{c}[{}^3P_J^{[1]}] + g + g, \\
Z &\rightarrow c\bar{c}[{}^3P_J^{[1]}] + c + \bar{c}.
\end{aligned} \tag{3}$$

The typical Feynman diagrams corresponding to Eqs. (2) and (3) are presented in Figs. 1, 2 and 3, including 51 diagrams for ${}^3S_1^{[8]}$ (2 LO diagrams, 6 counter-terms, 15 one-loop, 18 diagrams for real corrections and 10 NLO* diagrams) and 10 diagrams for ${}^3P_J^{[1]}$. Note that, as shown in Eq. (2), the real correction processes $Z \rightarrow c\bar{c}[{}^3S_1^{[8]}] + q + \bar{q}$ have been classified into two categorises, namely $q = u$ and $q = d(s)$, and in Fig.(1e), the diagrams involving fermion loops of u, c and d, s, b are also divided into two groups.

For purpose of isolating the ultraviolet (UV) and infrared (IR) divergences, we adopt the dimensional regularization with $D = 4 - 2\epsilon$. The on-mass-shell (OS) scheme is employed to set the renormalization constants for the heavy quark mass, the heavy quark field and gluon field, namely Z_m , Z_2 and Z_3 , respectively. The modified minimal-subtraction (\overline{MS}) scheme is adopted for the QCD gauge coupling, Z_g , ($Q = c, b$)

$$\begin{aligned}
\delta Z_m^{OS} &= -3C_F \frac{\alpha_s N_\epsilon}{4\pi} \left[\frac{1}{\epsilon_{UV}} - \gamma_E + \ln \frac{4\pi\mu_r^2}{m_Q^2} + \frac{4}{3} + \mathcal{O}(\epsilon) \right], \\
\delta Z_2^{OS} &= -C_F \frac{\alpha_s N_\epsilon}{4\pi} \left[\frac{1}{\epsilon_{UV}} + \frac{2}{\epsilon_{IR}} - 3\gamma_E + 3\ln \frac{4\pi\mu_r^2}{m_Q^2} \right. \\
&\quad \left. + 4 + \mathcal{O}(\epsilon) \right], \\
\delta Z_3^{\overline{MS}} &= \frac{\alpha_s N_\epsilon}{4\pi} [\beta_0(n_{lf}) - 2C_A] \left[\left(\frac{1}{\epsilon_{UV}} - \frac{1}{\epsilon_{IR}} \right) \right. \\
&\quad \left. - \frac{4}{3} T_F \left(\frac{1}{\epsilon_{UV}} - \gamma_E + \ln \frac{4\pi\mu_r^2}{m_c^2} \right) \right. \\
&\quad \left. - \frac{4}{3} T_F \left(\frac{1}{\epsilon_{UV}} - \gamma_E + \ln \frac{4\pi\mu_r^2}{m_b^2} \right) + \mathcal{O}(\epsilon) \right], \\
\delta Z_g^{\overline{MS}} &= -\frac{\beta_0(n_f)}{2} \frac{\alpha_s N_\epsilon}{4\pi} \left[\frac{1}{\epsilon_{UV}} - \gamma_E + \ln(4\pi) + \mathcal{O}(\epsilon) \right], \tag{4}
\end{aligned}$$

where γ_E is the Euler's constant, $\beta_0(n_f) = \frac{11}{3}C_A - \frac{4}{3}T_F n_f$ is the one-loop coefficient of the β -function, and $\beta_0(n_{lf})$ is identical to $\frac{11}{3}C_A - \frac{4}{3}T_F n_{lf}$, with $n_f (= 5)$ denoting the number of active quark flavors and light quark flavors respectively. $N_\epsilon = \Gamma[1 - \epsilon]/(4\pi\mu_r^2/(4m_c^2))^\epsilon$. In $SU(3)_c$, the color factors are given by $T_F = \frac{1}{2}$, $C_F = \frac{4}{3}$ and $C_A = 3$. To subtract the IR divergences in the real correction channels as listed in Eq. 2, the two cutoff slicing strategy [24] is utilized.

To calculate the D-dimension trace of the fermion loop involving γ_5 , under the scheme described in [25], we write down all the amplitudes from the same starting point (such as the Z -vertex) and abandon the cyclicity. As a crosscheck for the correctness of the treatments on γ_5 , we have calculated the QCD NLO corrections to the similar process, $Z \rightarrow c\bar{c}[{}^3S_1^{[1]}] + \gamma$, and obtain exactly the same K factor as in [26].

To deal with the color singlet (CS) processes, $Z \rightarrow c\bar{c}(b\bar{b})[{}^3P_J^{[1]}] + g + g$, which involve soft singularities, we first classify $\Gamma(Z \rightarrow c\bar{c}[{}^3P_J^{[1]}] + g + g)$ into two terms (the $b\bar{b}$ cases can

be obtained in a similar way),

$$d\Gamma(Z \rightarrow c\bar{c}[{}^3P_J^{[1]}] + g + g) = d\hat{\Gamma}_{3P_J^{[1]}}\langle\mathcal{O}^{\chi_c}({}^3P_J^{[1]})\rangle \\ + d\hat{\Gamma}_{3S_1^{[8]}}^{LO}\langle\mathcal{O}^{\chi_c}({}^3S_1^{[8]})\rangle^{NLO}, \quad (5)$$

then we have

$$d\hat{\Gamma}_{3P_J^{[1]}}\langle\mathcal{O}^{\chi_c}({}^3P_J^{[1]})\rangle = d\Gamma(Z \rightarrow c\bar{c}[{}^3P_J^{[1]}] + g + g) \\ - d\hat{\Gamma}_{3S_1^{[8]}}^{LO}\langle\mathcal{O}^{\chi_c}({}^3S_1^{[8]})\rangle^{NLO}. \quad (6)$$

Both $d\Gamma(Z \rightarrow c\bar{c}[{}^3P_J^{[1]}] + g + g)$ and $\langle\mathcal{O}^{\chi_c}({}^3S_1^{[8]})\rangle^{NLO}$ have IR singularities, which can cancel each other. The soft part of $d\Gamma(Z \rightarrow c\bar{c}[{}^3P_J^{[1]}] + g + g)$ can be written as (“ s ” means soft)

$$d\Gamma(Z \rightarrow c\bar{c}[{}^3P_J^{[1]}] + g + g)|_s = \\ -\frac{\alpha_s}{3\pi m_c}u_\epsilon^s \frac{N_c^2 - 1}{N_c} d\hat{\Gamma}_{3S_1^{[8]}}^{LO}\langle\mathcal{O}^{\chi_c}({}^3P_J^{[1]})\rangle \quad (7)$$

with

$$u_\epsilon^s = \frac{1}{\epsilon_{IR}} + \frac{E}{|\mathbf{p}|} \ln\left(\frac{E + |\mathbf{p}|}{E - |\mathbf{p}|}\right) + \ln\left(\frac{4\pi\mu_r^2}{s\delta_s^2}\right) - \gamma_E - \frac{1}{3}, \quad (8)$$

where N_c is identical to 3 for $SU(3)$ gauge field. E and \mathbf{p} denote the energy and 3-momentum of χ_c , respectively. δ_s is the usual “soft cut” employed to impose an amputation on the energy of the emitted gluon.

Now we are to calculate the transition rate of ${}^3S_1^{[8]}$ into ${}^3P_J^{[1]}$. Under the dimensional regularization scheme, we have

$$\langle\mathcal{O}^{\chi_c}({}^3S_1^{[8]})\rangle^{NLO} = -\frac{\alpha_s}{3\pi m_c}u_\epsilon^c \frac{N_c^2 - 1}{N_c} \langle\mathcal{O}^{\chi_c}({}^3P_J^{[1]})\rangle, \quad (9)$$

where, on the basis of μ_Λ -cutoff scheme, u_ϵ^c has the form of

$$u_\epsilon^c = \frac{1}{\epsilon_{IR}} - \gamma_E - \frac{1}{3} - \ln\left(\frac{4\pi\mu_r^2}{\mu_\Lambda^2}\right). \quad (10)$$

Substituting Eqs. (7), (8), (9) and (10) into Eq. (6), we finally obtain the finite short distance coefficient for ${}^3P_J^{[1]}$, namely $d\hat{\Gamma}_{3P_J^{[1]}}$. Having eliminated all the singularities, we will move on to perform the numerical calculations.

III. NUMERICAL RESULTS AND DISCUSSIONS

Before presenting the phenomenological results, we first demonstrate the choices of the parameters in our calculations. To keep the gauge invariance, the masses of χ_c and χ_b are set to be $2m_c$ and $2m_b$ respectively, with $m_c = 1.5 \pm 0.1$ GeV and $m_b = 4.9 \pm 0.2$ GeV. $m_Z = 91.1876$ GeV. $\alpha = 1/137$. In the calculations for the NLO, the NLO* and two $^3P_J^{[1]}$ processes, as listed in Eqs. (2) and (3), we employ the two-loop α_s running, and one-loop α_s running for LO. We take $m_c(m_b)$ as the value of μ_Λ for $\chi_c(\chi_b)$. The values of $\langle \mathcal{O}^{\chi_c(\chi_b)}(^3S_1^8) \rangle$ are taken as

$$\begin{aligned} \langle \mathcal{O}^{\chi_{c0}}(^3S_1^{[8]}) \rangle &= 2.15 \times 10^{-3} \text{ GeV}^3, \\ \langle \mathcal{O}^{\chi_{b0}}(^3S_1^{[8]}) \rangle &= 9.40 \times 10^{-3} \text{ GeV}^3, \end{aligned} \quad (11)$$

from Refs. [8] and [23]. In the case of $^3P_J^{[1]}$ channels, the relation $\langle \mathcal{O}^{\chi_{cJ}(\chi_{bJ})}(^3P_J^{[1]}) \rangle = \frac{9}{2\pi}(2J+1)|R'_p(0)|^2$ is adopted, where $|R'_p(0)|^2 = 0.075 \text{ GeV}^5$ for χ_c and 1.417 GeV^5 for χ_b .

In our calculations, the mathematica packages *Malt@FDC* are employed to deal with the virtual corrections, and *FDC* packages serve as the agent to evaluate the contributions from the hard non-collinear parts. Both the cancellation of divergence and the independence on cutoff have been checked carefully.

A. Phenomenological results for χ_c

The NRQCD predictions for $\Gamma(Z \rightarrow \chi_{cJ} + X)$ with $J = 0, 1, 2$ are demonstrated in Tables. I, II and III, respectively. One can see that the branching ratios for χ_c are on the order

TABLE I: The decay widths (unit: KeV) of $\Gamma(Z \rightarrow \chi_{c0} + X)$. $\mu_\Lambda = m_c$.

μ_r	$m_c(\text{GeV})$	$^3S_1^{[8]} _{\text{LO}}$	$^3S_1^{[8]} _{\text{NLO}}$	$^3S_1^{[8]} _{\text{NLO}^*}$	$^3P_0^{[1]} _{gg}$	$^3P_0^{[1]} _{c\bar{c}}$	Γ_{total}	$\text{Br}(10^{-5})$
$2m_c$	1.4	1.20×10^{-2}	14.9	8.26	5.63×10^{-2}	27.0	50.2	2.02
	1.5	1.09×10^{-2}	10.9	6.05	4.27×10^{-2}	18.1	35.1	1.41
	1.6	9.99×10^{-3}	8.12	4.53	3.30×10^{-2}	12.5	25.1	1.01
m_Z	1.4	5.30×10^{-3}	2.99	1.66	1.13×10^{-2}	5.43	10.1	0.41
	1.5	4.95×10^{-3}	2.31	1.28	9.06×10^{-3}	3.84	7.45	0.30
	1.6	4.64×10^{-3}	1.82	1.01	7.36×10^{-3}	2.78	5.61	0.23

TABLE II: The decay widths (unit: KeV) of $\Gamma(Z \rightarrow \chi_{c1} + X)$. $\mu_\Lambda = m_c$.

μ_r	$m_c(\text{GeV})$	$^3S_1^{[8]} _{\text{LO}}$	$^3S_1^{[8]} _{\text{NLO}}$	$^3S_1^{[8]} _{\text{NLO}^*}$	$^3P_1^{[1]} _{gg}$	$^3P_1^{[1]} _{c\bar{c}}$	Γ_{total}	$\text{Br}(10^{-5})$
$2m_c$	1.4	3.60×10^{-2}	44.6	24.8	1.47	29.9	101	4.06
	1.5	3.27×10^{-2}	32.6	18.2	1.09	20.0	71.9	2.89
	1.6	3.00×10^{-2}	24.4	13.6	0.819	13.7	52.5	2.11
m_Z	1.4	1.59×10^{-2}	8.98	4.98	0.296	6.01	20.3	0.82
	1.5	1.49×10^{-2}	6.94	3.85	0.231	4.23	15.3	0.61
	1.6	1.39×10^{-2}	5.45	3.03	0.183	3.05	11.7	0.47

 TABLE III: The decay widths (unit: KeV) of $\Gamma(Z \rightarrow \chi_{c2} + X)$. $\mu_\Lambda = m_c$.

μ_r	$m_c(\text{GeV})$	$^3S_1^{[8]} _{\text{LO}}$	$^3S_1^{[8]} _{\text{NLO}}$	$^3S_1^{[8]} _{\text{NLO}^*}$	$^3P_2^{[1]} _{gg}$	$^3P_2^{[1]} _{c\bar{c}}$	Γ_{total}	$\text{Br}(10^{-5})$
$2m_c$	1.4	6.00×10^{-2}	74.3	41.3	1.03	11.7	128	5.14
	1.5	5.46×10^{-2}	54.4	30.3	0.780	7.84	93.2	3.74
	1.6	4.99×10^{-2}	40.6	22.6	0.601	5.39	69.2	2.78
m_Z	1.4	2.65×10^{-2}	15.0	8.30	0.208	2.35	25.8	1.04
	1.5	2.48×10^{-2}	11.6	6.42	0.166	1.66	19.8	0.80
	1.6	2.32×10^{-2}	9.08	5.05	0.134	1.20	15.5	0.62

of 10^{-5} . To be specific, considering the uncertainties induced by the choices of the values of μ_r and m_c , we have

$$\begin{aligned}
 \text{Br}(Z \rightarrow \chi_{c0} + X) &= (0.23 - 2.02) \times 10^{-5}, \\
 \text{Br}(Z \rightarrow \chi_{c1} + X) &= (0.47 - 4.06) \times 10^{-5}, \\
 \text{Br}(Z \rightarrow \chi_{c2} + X) &= (0.62 - 5.14) \times 10^{-5},
 \end{aligned} \tag{12}$$

which signifies a detectable prospect of these decay processes at LHC or other platforms. It is observed that the QCD NLO corrections can enhance the LO results significantly, by 2 – 3 orders, which can be attributed to the kinematic enhancements via the $^3S_1^{[8]}$ single gluon fragmentation (SGF) diagrams that emerge first at the NLO level, such as the one-loop triangle anomalous diagrams (Fig. 1(e)) and those (Fig. 1(j)) associated with a final $q\bar{q}$ ($q = u, d, s$) pair. By the same token, the NLO* channels can also provide considerable contributions, about one half of the NLO results. Consequently the CO channels will play

a vital role in the decay processes of $Z \rightarrow \chi_c + X$. To show the CO significance evidently, we introduce the following ratios

$$\begin{aligned}\Gamma_{CO}^{\chi_{c0}}/\Gamma_{\text{total}}^{\chi_{c0}} &= (46.1 - 50.3)\%, \\ \Gamma_{CO}^{\chi_{c1}}/\Gamma_{\text{total}}^{\chi_{c1}} &= (68.9 - 72.4)\%, \\ \Gamma_{CO}^{\chi_{c2}}/\Gamma_{\text{total}}^{\chi_{c2}} &= (90.1 - 91.4)\%,\end{aligned}\tag{13}$$

where $\Gamma_{CO}^{\chi_{cJ}}$ ($J = 0, 1, 2$) denotes the sum of the contributions from NLO and NLO*, and $\Gamma_{\text{total}}^{\chi_{cJ}}$ is the total results by adding together the CO and CS contributions. In addition to the crucial impacts on the total widths, the CO channels are also capable of significantly influencing the predictions on the ratios of χ_{c1}/χ_{c0} and χ_{c2}/χ_{c0} , as shown below

$$\begin{aligned}\text{CS} : \quad \Gamma_{\chi_{c1}}/\Gamma_{\chi_{c0}} &= 1.159 - 1.162, \\ \text{NRQCD} : \quad \Gamma_{\chi_{c1}}/\Gamma_{\chi_{c0}} &= 2.007 - 2.087, \\ \text{CS} : \quad \Gamma_{\chi_{c2}}/\Gamma_{\chi_{c0}} &= 0.471 - 0.480, \\ \text{NRQCD} : \quad \Gamma_{\chi_{c2}}/\Gamma_{\chi_{c0}} &= 2.558 - 2.756.\end{aligned}\tag{14}$$

One can see that the CS results have been thoroughly changed by the inclusion of the CO states. These conspicuous differences can be regarded as an outstanding probe to distinguish the CO and CS mechanism.

On the aspect of CS, the c quark fragmentation dominated channels, namely $Z \rightarrow c\bar{c}[{}^3P_J^{[1]}] + c + \bar{c}$, serve as the leading role, and $Z \rightarrow c\bar{c}[{}^3P_J^{[1]}] + g + g$ contribute moderately, about 0.24%, 5% and 10% of the total CS predictions, corresponding to $J = 0, 1, 2$ respectively.

As was pointed out in the introduction to this paper, the χ_c feeddown may have a substantial impact on the production of J/ψ . Therefore we employ the branching ratios of χ_c to J/ψ as listed in [27], specifically $\text{Br}(\chi_{c0} \rightarrow J/\psi + \gamma) = 1.4\%$, $\text{Br}(\chi_{c1} \rightarrow J/\psi + \gamma) = 34.3\%$ and $\text{Br}(\chi_{c2} \rightarrow J/\psi + \gamma) = 19.0\%$, to evaluate $\Gamma(Z \rightarrow J/\psi + X)$ via the χ_c feeddown. Summing over all the contributions from χ_{c0} , χ_{c1} and χ_{c2} , we finally obtain

$$\Gamma(Z \rightarrow J/\psi + X)|_{\chi_c\text{-feeddown}} = (0.28 \sim 2.4) \times 10^{-5},\tag{15}$$

which is about one order of magnitude smaller than the experimental data released from the L3 Collaboration at LEP [28].

B. Phenomenological results for χ_b

TABLE IV: The decay widths (unit: KeV) of $\Gamma(Z \rightarrow \chi_{b0} + X)$. $\mu_\Lambda = m_b$.

μ_r	$m_b(\text{GeV})$	$^3S_1^{[8]} _{\text{LO}}$	$^3S_1^{[8]} _{\text{NLO}}$	$^3S_1^{[8]} _{\text{NLO}^*}$	$^3P_0^{[1]} _{gg}$	$^3P_0^{[1]} _{b\bar{b}}$	Γ_{total}	$\text{Br}(10^{-7})$
$2m_b$	4.7	9.76×10^{-3}	0.272	0.148	8.84×10^{-3}	0.677	1.11	4.46
	4.9	9.26×10^{-3}	0.225	0.121	7.46×10^{-3}	0.535	0.888	3.57
	5.1	8.82×10^{-3}	0.187	9.95×10^{-2}	6.34×10^{-3}	0.426	0.719	2.89
m_Z	4.7	6.34×10^{-3}	0.119	6.26×10^{-2}	3.74×10^{-3}	0.286	0.472	1.90
	4.9	6.08×10^{-3}	0.101	5.22×10^{-2}	3.22×10^{-3}	0.231	0.387	1.55
	5.1	5.85×10^{-3}	8.62×10^{-2}	4.37×10^{-2}	2.79×10^{-3}	0.187	0.320	1.29

TABLE V: The decay widths (unit: KeV) of $\Gamma(Z \rightarrow \chi_{b1} + X)$. $\mu_\Lambda = m_b$.

μ_r	$m_b(\text{GeV})$	$^3S_1^{[8]} _{\text{LO}}$	$^3S_1^{[8]} _{\text{NLO}}$	$^3S_1^{[8]} _{\text{NLO}^*}$	$^3P_1^{[1]} _{gg}$	$^3P_1^{[1]} _{b\bar{b}}$	Γ_{total}	$\text{Br}(10^{-7})$
$2m_b$	4.7	2.92×10^{-2}	0.814	0.445	0.153	0.653	2.06	8.28
	4.9	2.78×10^{-2}	0.674	0.362	0.128	0.512	1.68	6.74
	5.1	2.64×10^{-2}	0.562	0.299	0.109	0.405	1.37	5.50
m_Z	4.7	1.90×10^{-2}	0.357	0.188	6.47×10^{-2}	0.276	0.886	3.56
	4.9	1.83×10^{-2}	0.303	0.157	5.54×10^{-2}	0.221	0.736	2.96
	5.1	1.75×10^{-2}	0.258	0.131	4.77×10^{-2}	0.178	0.616	2.47

Based on NRQCD, the predicted decay widths via $Z \rightarrow \chi_{bJ} + X$ are presented in Tables. IV, V and VI, corresponding to $J = 0, 1, 2$, respectively. From the data in the three Tables, it is apparent that the branching ratio for $Z \rightarrow \chi_{bJ} + X$ is about one or two orders of magnitudes smaller than that of χ_c , around $10^{-7} - 10^{-6}$. Taking into account the uncertainties induced by μ_r and the mass of b quark, we have

$$\begin{aligned}
\text{Br}(Z \rightarrow \chi_{b0} + X) &= (1.29 - 4.46) \times 10^{-7}, \\
\text{Br}(Z \rightarrow \chi_{b1} + X) &= (2.47 - 8.28) \times 10^{-7}, \\
\text{Br}(Z \rightarrow \chi_{b2} + X) &= (0.31 - 1.02) \times 10^{-6}.
\end{aligned} \tag{16}$$

Similar to the case of χ_c , the NLO QCD corrections can also enlarge the LO results significantly, by about 10-20 times, and the impact of NLO* channels are as always sizeable. The

TABLE VI: The decay widths (unit: KeV) of $\Gamma(Z \rightarrow \chi_{b2} + X)$. $\mu_\Lambda = m_b$.

μ_r	$m_b(\text{GeV})$	$^3S_1^{[8]} _{\text{LO}}$	$^3S_1^{[8]} _{\text{NLO}}$	$^3S_1^{[8]} _{\text{NLO}^*}$	$^3P_2^{[1]} _{gg}$	$^3P_2^{[1]} _{b\bar{b}}$	Γ_{total}	$\text{Br}(10^{-7})$
$2m_b$	4.7	4.88×10^{-2}	1.360	0.743	0.160	0.270	2.53	10.2
	4.9	4.63×10^{-2}	1.130	0.605	0.136	0.212	2.08	8.35
	5.1	4.41×10^{-2}	0.937	0.497	0.116	0.168	1.72	6.91
m_Z	4.7	3.18×10^{-2}	0.595	0.312	6.78×10^{-2}	0.114	1.09	4.38
	4.9	3.04×10^{-2}	0.504	0.261	5.87×10^{-2}	9.12×10^{-2}	0.915	3.69
	5.1	2.92×10^{-2}	0.430	0.219	5.12×10^{-2}	7.36×10^{-2}	0.774	3.11

ratios of the CO contributions to the total widths are slightly smaller than the χ_c cases, to be specific

$$\begin{aligned}
 \Gamma_{CO}^{\chi_{b0}}/\Gamma_{\text{total}}^{\chi_{b0}} &= (37.8 - 40.6)\%, \\
 \Gamma_{CO}^{\chi_{b1}}/\Gamma_{\text{total}}^{\chi_{b1}} &= (51.5 - 63.3)\%, \\
 \Gamma_{CO}^{\chi_{b2}}/\Gamma_{\text{total}}^{\chi_{b2}} &= (83.0 - 83.9)\%,
 \end{aligned} \tag{17}$$

where $\Gamma_{CO}^{\chi_{bJ}}$, with $J = 0, 1, 2$, represents the sum of the NLO and NLO* contributions, and $\Gamma_{\text{total}}^{\chi_{bJ}}$ denotes the total widths, including both the CO and CS effects. The relative smallness of these ratios can be partly ascribed to that the larger mass of m_b will weaken the significance of the enhancements via SGF. Regarding the ratios of χ_{b1}/χ_{b0} and χ_{b2}/χ_{b0} , the NRQCD predictions are still far different from those built on the CS mechanism, namely

$$\begin{aligned}
 \text{CS} : \quad \Gamma_{\chi_{b1}}/\Gamma_{\chi_{b0}} &= 1.175 - 1.188, \\
 \text{NRQCD} : \quad \Gamma_{\chi_{b1}}/\Gamma_{\chi_{b0}} &= 1.868 - 1.923, \\
 \text{CS} : \quad \Gamma_{\chi_{b2}}/\Gamma_{\chi_{b0}} &= 0.626 - 0.657, \\
 \text{NRQCD} : \quad \Gamma_{\chi_{b2}}/\Gamma_{\chi_{b0}} &= 2.286 - 2.420.
 \end{aligned} \tag{18}$$

Analogous to χ_c , the dissimilarities between these ratios are also very beneficial to check the validity of the CO mechanism.

In contrast to the previously stated “moderation” of the effects via $Z \rightarrow c\bar{c}[^3P_J^{[1]}] + g + g$, in the case of χ_b , the channel $Z \rightarrow b\bar{b}[^3P_J^{[1]}] + g + g$ can provide remarkable contributions,

namely

$$\begin{aligned}
\Gamma_{3P_0^{[1]}}^{gg}/\Gamma_{3P_0^{[1]}}^{\text{CS}} &\sim 1.5\%, \\
\Gamma_{3P_1^{[1]}}^{gg}/\Gamma_{3P_1^{[1]}}^{\text{CS}} &\sim 20\%, \\
\Gamma_{3P_2^{[1]}}^{gg}/\Gamma_{3P_2^{[1]}}^{\text{CS}} &\sim 40\%,
\end{aligned} \tag{19}$$

where, corresponding to $J = 0, 1, 2$ respectively, the label $\Gamma_{3P_J^{[1]}}^{gg}$ refers to $\Gamma(Z \rightarrow b\bar{b}[{}^3P_J^{[1]}] + g + g)$, and $\Gamma_{3P_J^{[1]}}^{\text{CS}}$ is for the sum of $\Gamma(Z \rightarrow b\bar{b}[{}^3P_J^{[1]}] + g + g)$ and $\Gamma(Z \rightarrow b\bar{b}[{}^3P_J^{[1]}] + b + \bar{b})$. It is worth mentioning that, to satisfy the conservation of C -parity, at B factories, the processes $e^+e^- \rightarrow \gamma^* \rightarrow c\bar{c}(b\bar{b})[{}^3P_J^{[1]}] + g + g$ are forbidden, leaving alone the heavy quark pair associated channels as the unique CS processes. Moreover the center-of-mass energy at B factories, namely 10.6 GeV, is too small to allow for $e^+e^- \rightarrow \gamma^* \rightarrow (b\bar{b})[{}^3P_J^{[1]}] + b\bar{b}$. From these points of view, the decay of Z boson seems to be more suitable for studying χ_c and χ_b .

At last, as a further step towards providing a sound estimate on the $\Upsilon(1S)$ production via Z decay, we make use of the branching ratios of χ_b to $\Upsilon(1S)$, namely $\text{Br}(\chi_{b0} \rightarrow \Upsilon(1S) + \gamma) = 1.94\%$, $\text{Br}(\chi_{b1} \rightarrow \Upsilon(1S) + \gamma) = 35.0\%$ and $\text{Br}(\chi_{b2} \rightarrow \Upsilon(1S) + \gamma) = 18.8\%$, to calculate the impact of the χ_b feeddown on $\Gamma(Z \rightarrow \Upsilon(1S) + X)$. Taking into account all the contributions from χ_{b0} , χ_{b1} and χ_{b2} , we finally obtain

$$\Gamma(Z \rightarrow \Upsilon(1S) + X)|_{\chi_b\text{-feeddown}} = (0.15 \sim 0.49) \times 10^{-6}. \tag{20}$$

IV. SUMMARY

In this paper, we have systematically investigated the decay of Z boson into χ_c and χ_b , respectively. It is found that the branching ratio for $Z \rightarrow \chi_c + X$ is on the order of 10^{-5} , and 10^{-6} for the χ_b case, which implies that these decay processes are able to be detected. It is observed that, the ${}^3S_1^{[8]}$ SGF diagrams that first emerge at the NLO level will significantly enhance the LO results by about 2-3 orders for $c\bar{c}$, and 10-20 times for $b\bar{b}$. For the same reasons, the NLO* processes can also contribute considerably, about 50% of the NLO results. Consequently, the CO contributions will play a vital, even dominant, role in the decay processes, $Z \rightarrow \chi_c(\chi_b) + X$. Aside from the significance in the total widths, the ${}^3S_1^{[8]}$ state also has a remarkable effect on the predictions on the ratios of $\Gamma(\chi_{c2})/\Gamma(\chi_{c0})$,

$\Gamma(\chi_{c1})/\Gamma(\chi_{c0})$, $\Gamma(\chi_{b1})/\Gamma(\chi_{b0})$ and $\Gamma(\chi_{b2})/\Gamma(\chi_{b0})$, thoroughly changeing the results based on the CS mechanism. On the aspect of CS, the heavy quark pair associated channels, namely $Z \rightarrow Q\bar{Q}[{}^3P_J^{[1]}] + Q\bar{Q}$, play a leading role, however, the processes $Z \rightarrow Q\bar{Q}[{}^3P_J^{[1]}] + gg$ can also provide significant contributions, especially for χ_b . Taking into considerations the χ_{cJ} and χ_{bJ} feeddown contributions respectively, we find $\Gamma(Z \rightarrow J/\psi + X)|_{\chi_c\text{-feeddown}} = (0.28 - 2.4) \times 10^{-5}$ and $\Gamma(Z \rightarrow \Upsilon(1S) + X)|_{\chi_b\text{-feeddown}} = (0.15 - 0.49) \times 10^{-6}$. In summary, the decay of Z boson into $\chi_c(\chi_b)$ can be regarded as an ideal laboratory to further identify the significance of color octet mechanism.

V. ACKNOWLEDGMENTS

Acknowledgments: We would like to thank Wen-Long Sang for helpful discussions on the treatments on γ_5 . This work is supported in part by the Natural Science Foundation of China under the Grant No.11705034., by the Project for Young Talents Growth of Guizhou Provincial Department of Education under Grant No.KY[2017]135, and the Key Project for Innovation Research Groups of Guizhou Provincial Department of Education under Grant No.KY[2016]028.

-
- [1] G. T. Bodwin, E. Braaten and G. P. Lepage, “Rigorous QCD analysis of inclusive annihilation and production of heavy quarkonium, Phys. Rev. D **51** (1995) 1125 Erratum: [Phys. Rev. D **55** (1997) 5853] doi:10.1103/PhysRevD.55.5853, 10.1103/PhysRevD.51.1125.
 - [2] E. Braaten and S. Fleming, Color octet fragmentation and the psi-prime surplus at the Tevatron, Phys. Rev. Lett. **74** (1995) 3327 doi:10.1103/PhysRevLett.74.3327.
 - [3] P. L. Cho and A. K. Leibovich, Color octet quarkonia production, Phys. Rev. D **53** (1996) 150 doi:10.1103/PhysRevD.53.150.
 - [4] P. L. Cho and A. K. Leibovich, Color octet quarkonia production. 2., Phys. Rev. D **53** (1996) 6203 doi:10.1103/PhysRevD.53.6203.
 - [5] H. Han, Y. Q. Ma, C. Meng, H. S. Shao and K. T. Chao, η_c production at LHC and indications on the understanding of J/ψ production, Phys. Rev. Lett. **114** (2015) no.9, 092005

- doi:10.1103/PhysRevLett.114.092005.
- [6] H. F. Zhang, Z. Sun, W. L. Sang and R. Li, Impact of η_c hadroproduction data on charmonium production and polarization within NRQCD framework, Phys. Rev. Lett. **114** (2015) no.9, 092006 doi:10.1103/PhysRevLett.114.092006.
 - [7] B. Gong, L. P. Wan, J. X. Wang and H. F. Zhang, Complete next-to-leading-order study on the yield and polarization of $\Upsilon(1S, 2S, 3S)$ at the Tevatron and LHC, Phys. Rev. Lett. **112** (2014) no.3, 032001 doi:10.1103/PhysRevLett.112.032001.
 - [8] Y. Feng, B. Gong, L. P. Wan and J. X. Wang, An updated study of Υ production and polarization at the Tevatron and LHC, Chin. Phys. C **39** (2015) no.12, 123102 doi:10.1088/1674-1137/39/12/123102.
 - [9] K. Wang, Y. Q. Ma and K. T. Chao, $\Upsilon(1S)$ prompt production at the Tevatron and LHC in nonrelativistic QCD, Phys. Rev. D **85** (2012) 114003 doi:10.1103/PhysRevD.85.114003.
 - [10] H. Han, Y. Q. Ma, C. Meng, H. S. Shao, Y. J. Zhang and K. T. Chao, $\Upsilon(nS)$ and $\chi_b(nP)$ production at hadron colliders in nonrelativistic QCD, Phys. Rev. D **94** (2016) no.1, 014028 doi:10.1103/PhysRevD.94.014028.
 - [11] M. Butenschoen and B. A. Kniehl, Complete next-to-leading-order corrections to J/ψ photoproduction in nonrelativistic quantum chromodynamics, Phys. Rev. Lett. **104** (2010) 072001 doi:10.1103/PhysRevLett.104.072001.
 - [12] Z. Sun and H. F. Zhang, QCD corrections to the color-singlet J/ψ production in deeply inelastic scattering at HERA, Phys. Rev. D **96** (2017) no.9, 091502 doi:10.1103/PhysRevD.96.091502.
 - [13] Z. Sun and H. F. Zhang, QCD leading order study of the J/ψ leptonproduction at HERA within the nonrelativistic QCD framework, Eur. Phys. J. C **77** (2017) no.11, 744 doi:10.1140/epjc/s10052-017-5323-6.
 - [14] Y. J. Zhang, Y. Q. Ma, K. Wang and K. T. Chao, QCD radiative correction to color-octet J/ψ inclusive production at B Factories, Phys. Rev. D **81** (2010) 034015 doi:10.1103/PhysRevD.81.034015.
 - [15] M. Butenschoen and B. A. Kniehl, J/ψ polarization at Tevatron and LHC: Nonrelativistic-QCD factorization at the crossroads, Phys. Rev. Lett. **108** (2012) 172002 doi:10.1103/PhysRevLett.108.172002.
 - [16] K. T. Chao, Y. Q. Ma, H. S. Shao, K. Wang and Y. J. Zhang, J/ψ Polariza-

- tion at Hadron Colliders in Nonrelativistic QCD, Phys. Rev. Lett. **108** (2012) 242004 doi:10.1103/PhysRevLett.108.242004.
- [17] B. Gong, L. P. Wan, J. X. Wang and H. F. Zhang, Polarization for Prompt J/ψ and $(2s)$ Production at the Tevatron and LHC, Phys. Rev. Lett. **110** (2013) no.4, 042002 doi:10.1103/PhysRevLett.110.042002.
- [18] E. Braaten, B. A. Kniehl and J. Lee, Polarization of prompt J/ψ at the Tevatron, Phys. Rev. D **62** (2000) 094005 doi:10.1103/PhysRevD.62.094005.
- [19] R. Sharma and I. Vitev, High transverse momentum quarkonium production and dissociation in heavy ion collisions, Phys. Rev. C **87** (2013) no.4, 044905 doi:10.1103/PhysRevC.87.044905.
- [20] H. S. Shao, Y. Q. Ma, K. Wang and K. T. Chao, Polarizations of χ_{c1} and χ_{c2} in prompt production at the LHC, Phys. Rev. Lett. **112** (2014) no.18, 182003 doi:10.1103/PhysRevLett.112.182003.
- [21] D. Li, Y. Q. Ma and K. T. Chao, χ_{cJ} production associated with a $c\bar{c}$ pair at hadron colliders, Phys. Rev. D **83** (2011) 114037 doi:10.1103/PhysRevD.83.114037.
- [22] Y. Q. Ma, K. Wang and K. T. Chao, QCD radiative corrections to χ_{cJ} production at hadron colliders, Phys. Rev. D **83** (2011) 111503 doi:10.1103/PhysRevD.83.111503.
- [23] H. F. Zhang, L. Yu, S. X. Zhang and L. Jia, Global analysis of the experimental data on χ_c meson hadroproduction, Phys. Rev. D **93** (2016) no.5, 054033 Addendum: [Phys. Rev. D **93** (2016) no.7, 079901] doi:10.1103/PhysRevD.93.054033, 10.1103/PhysRevD.93.079901.
- [24] B. W. Harris and J. F. Owens, The Two cutoff phase space slicing method, Phys. Rev. D **65** (2002) 094032 doi:10.1103/PhysRevD.65.094032.
- [25] J. G. Korner, D. Kreimer and K. Schilcher, A Practicable gamma(5) scheme in dimensional regularization, Z. Phys. C **54** (1992) 503. doi:10.1007/BF01559471.
- [26] X. P. Wang and D. Yang, The leading twist light-cone distribution amplitudes for the S-wave and P-wave quarkonia and their applications in single quarkonium exclusive productions, JHEP **1406** (2014) 121 doi:10.1007/JHEP06(2014)121.
- [27] M. Tanabashi *et al.*, Review of Particle Physics, Phys. Rev. D **98** (2018) no.3, 030001. doi:10.1103/PhysRevD.98.030001.
- [28] M. Acciarri *et al.* [L3 Collaboration], Heavy quarkonium production in Z decays, Phys. Lett. B **453** (1999) 94. doi:10.1016/S0370-2693(99)00280-4.